

HNPS Advances in Nuclear Physics

Vol 30 (2024)

HNPS2023

HNPS: Advances in Nuclear Physics

31st Hellenic Conference

Editors: M. Diakaki, M. Kokkoris, V. Michalopoulou, R. Vlastou

HNPS: Advances in Nuclear Physics

Editors
M. Diakaki
M. Kokkoris
V. Michalopoulou
R. Vlastou

Proceedings of the
31st Hellenic
Conference
on Nuclear Physics

National Technical
University of Athens
Sep 29th - Sep 30th 2023

Hellenic Nuclear
Physics Society

**Detailed Study of the Reaction Mechanisms of ^{86}Kr
+ ^{64}Ni at 15 MeV/nucleon**

Olga Fasoula, G. A. Souliotis, S. Koulouris, M. Veselsky, S. J. Yenello, A. Bonasera

doi: [10.12681/hnpsanp.6271](https://doi.org/10.12681/hnpsanp.6271)

Copyright © 2024, Olga Fasoula, G. A. Souliotis, S. Koulouris, M. Veselsky, S. J. Yenello, A. Bonasera



This work is licensed under a [Creative Commons Attribution-NonCommercial-NoDerivatives 4.0](https://creativecommons.org/licenses/by-nc-nd/4.0/).

To cite this article:

Fasoula, O., G. A. Souliotis, S. Koulouris, M. Veselsky, S. J. Yenello, & A. Bonasera. (2024). Detailed Study of the Reaction Mechanisms of ^{86}Kr + ^{64}Ni at 15 MeV/nucleon. *HNPS Advances in Nuclear Physics*, 30, 181–184.
<https://doi.org/10.12681/hnpsanp.6271>

Detailed Study of the Reaction Mechanisms of $^{86}\text{Kr} + ^{64}\text{Ni}$ at 15 MeV/nucleon

O. Fasoula^{1,*}, G.A. Souliotis¹, S. Koulouris¹, M. Veselsky², S.J. Yenello³, A. Bonasera³

¹ Laboratory of Physical Chemistry, Department of Chemistry, National and Kapodistrian University of Athens, Zografou GR-15771, Greece

² Institute of Experimental and Applied Physics, Czech Technical University, Prague, Czech Republic

³ Cyclotron Institute, Texas A&M University, College Station, Texas, USA

Abstract We present a detailed study of momentum distributions of projectile fragments from the reaction $^{86}\text{Kr} + ^{64}\text{Ni}$ at 15 MeV/nucleon. The experimental data were obtained in previous work with the MARS separator at the Cyclotron Institute of Texas A&M University. Detailed calculations and the momentum distributions of ejectiles are presented and compared with the experimental data. The DIT and CoMD models are used for the dynamical part of the reaction and GEMINI is used for the de-excitation of the primary fragments. Our focus is on channels corresponding to the production of neutron rich nuclei. Both DIT and CoMD show promising results in the description of the experimental data, but further developments may be necessary. Through the systematic study of the momentum distributions, we try to elucidate the reaction mechanisms that dominate the production of neutron rich nuclei in the Fermi energy region.

Keywords Momentum Distributions, Multinucleon Transfer, Neutron-rich Nuclei, Fermi energy

INTRODUCTION

The study of nuclei in regions far from β -stability toward the neutron dripline is a fundamental issue for the nuclear physics community [1]. Multinucleon transfer reactions at energies near and below the Fermi energy (15-35 MeV/nucleon) are an effective means of reaching these neutron rich nuclei [2-5]. A substantial part of our research is directed toward the systematic study of momentum distribution of ejectiles from reactions of an ^{86}Kr beam at 15 and 25 MeV/nucleon with targets of Ni and Sn. We previously presented [6] mass, angular and momentum distributions of the reaction 15 MeV/nucleon ^{86}Kr with ^{64}Ni and compared them with model calculations. In this paper, we move forward in our study, and we present several reaction channels and detailed calculations with high statistics.

EXPERIMENTAL DATA AND THEORETICAL MODELS

The experimental data for this reaction were collected in this work [7] with the Momentum Achromat Recoil Separator (MARS) at the Cyclotron Institute at Texas A&M University. The data were collected within two angular ranges relative to the axis of the spectrometer: $2.2^\circ - 5.8^\circ$ (4° data) and $5.6^\circ - 9.2^\circ$ (7° data). The grazing angle for the reaction $^{86}\text{Kr} + ^{64}\text{Ni}$ at 15 MeV/nucleon is 6° so, the 4° data are expected to be the optimum setting. Therefore, in this work we present momentum distributions of the 4° data along with model calculations.

The calculations are based on a two-stage Monte Carlo approach. The phenomenological Deep Inelastic Transfer (DIT) model [8] and the microscopic Constrained Molecular Dynamics (CoMD) model [9,10] were used to simulate the interaction between the projectile and the target that leads to the production of excited projectile-like and target-like fragments. After the interaction, we focus on the excited projectile-like fragments, and we use the GEMINI code [11,12] for the de-excitation of these fragments. From now on, the DIT/GEMINI and CoMD/GEMINI calculations are referred to as DIT

* Corresponding author: olgas@chem.uoa.gr

and CoMD calculations, respectively.

MOMENTUM DISTRIBUTIONS

To begin with, we provide some information on momentum distributions. In the figures that follow, each panel represents a specific isotope and the corresponding momentum per nucleon (p/A) and differential cross sections ($d^2\sigma/d(p/A)d\Omega$ - [mb/(MeV/c)msr]). The vertical (green) dashed line is the p/A of the projectile. The experimental data exhibit various tendencies depending on the reaction channel. Generally, we observe a sharper quasielastic peak near the p/A of the beam and broader peaks as p/A decreases. The dips observed on the experimental distributions are the result of software gating of the elastically scattered ^{86}Kr projectiles. Specifically, by adjusting the “momentum” slits at the dispersive image of the separator the charge states of the elastically scattered beam were restricted from reaching the end detector [7]. Some peaks are shown with the total excitation energy of the dinuclear system (quasiprojectile-quasitarget) extracted by binary kinematics calculations.

Inelastic Channel

In Fig. 1 we present the inelastic channel of the reaction 15 MeV/nucleon $^{86}\text{Kr} + ^{64}\text{Ni}$ along with DIT (blue symbols) and CoMD (red symbols) calculations, right and left plot respectively. The CoMD calculation follows the shape of the broader peaks (especially for P/A values lower than 155 MeV/c) to a better degree than the DIT calculation but is higher than the quasielastic peak. The DIT calculation yields lower values of differential cross sections than the data but follows the overall shape of the p/A distributions.

Furthermore, we present a quasiprojectile analysis on the DIT calculation. This is based on the hypothesis that the ejectiles come from different quasiprojectiles after the pickup and the subsequent evaporation of zero neutrons, QP-0N (green squares), one neutron, QP-1N (purple diamonds) and two neutrons QP-2N (yellow triangles). We are currently in the process of assessing these distributions and their respective contribution in the total DIT calculation.

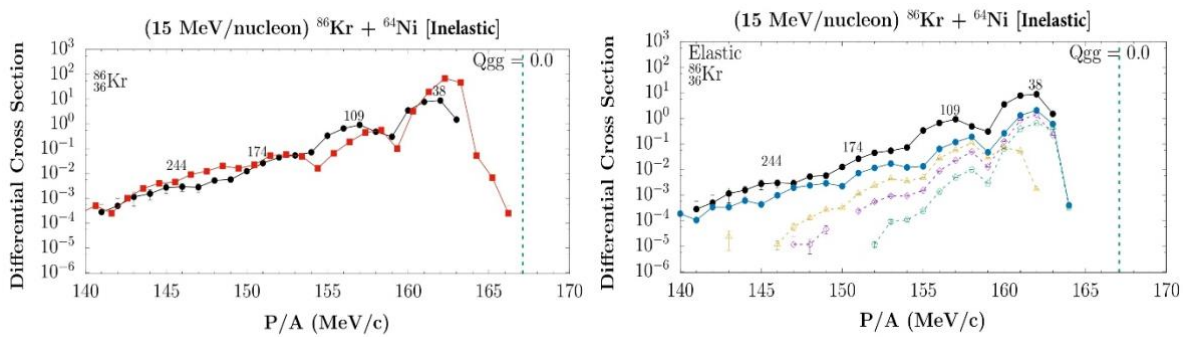


Figure 1. Momentum per nucleon distributions of ejectiles from the inelastic channel from $^{86}\text{Kr} + ^{64}\text{Ni}$ (15 MeV/nucleon). y-axis units: $(d^2\sigma/d(p/A)d\Omega$ - [mb/(MeV/c)msr]. Both panels: Experimental data: closed (black) circles. Numbers on top of peaks: Total excitation energy of dinuclear (quasitarget - quasiprojectile) system. Left panel: CoMD calculations closed (red) squares. Right panel: DIT calculations closed (blue) circles. DIT QP-0N: open (green) squares. DIT QP-1N: open (purple) diamonds. DIT QP-2N: open (yellow) triangles. The vertical dashed (green) line is the p/A of the projectile.

Neutron Pickup and Neutron Removal Channels

In Fig. 2 we present neutron pickup channels (+1n to +4n) on the left side and proton removal channels (-1p to -4p) on the right side. Similar observations can be made for these channels. On the

neutron pickup channels, the CoMD calculations are in better agreement with the data especially in lower p/A values even though both calculations tend to be lower than the data.

As for the proton removal channels, while the DIT calculations are still lower than the data, the CoMD calculations again seem to follow the broader peaks and to adequately describe the quasielastic region especially on the -2p and -3p channels.

On both channels as we move on to the addition or removal of more nucleons, we also move on to lower cross sections and more exotic nuclei. Both models yield fewer data points on these channels in part since these interactions are more complicated and there is need for further honing of the different parameters of the models. Also, to some degree, there is a need for greater statistics and longer run time for the calculations to reach these regions.

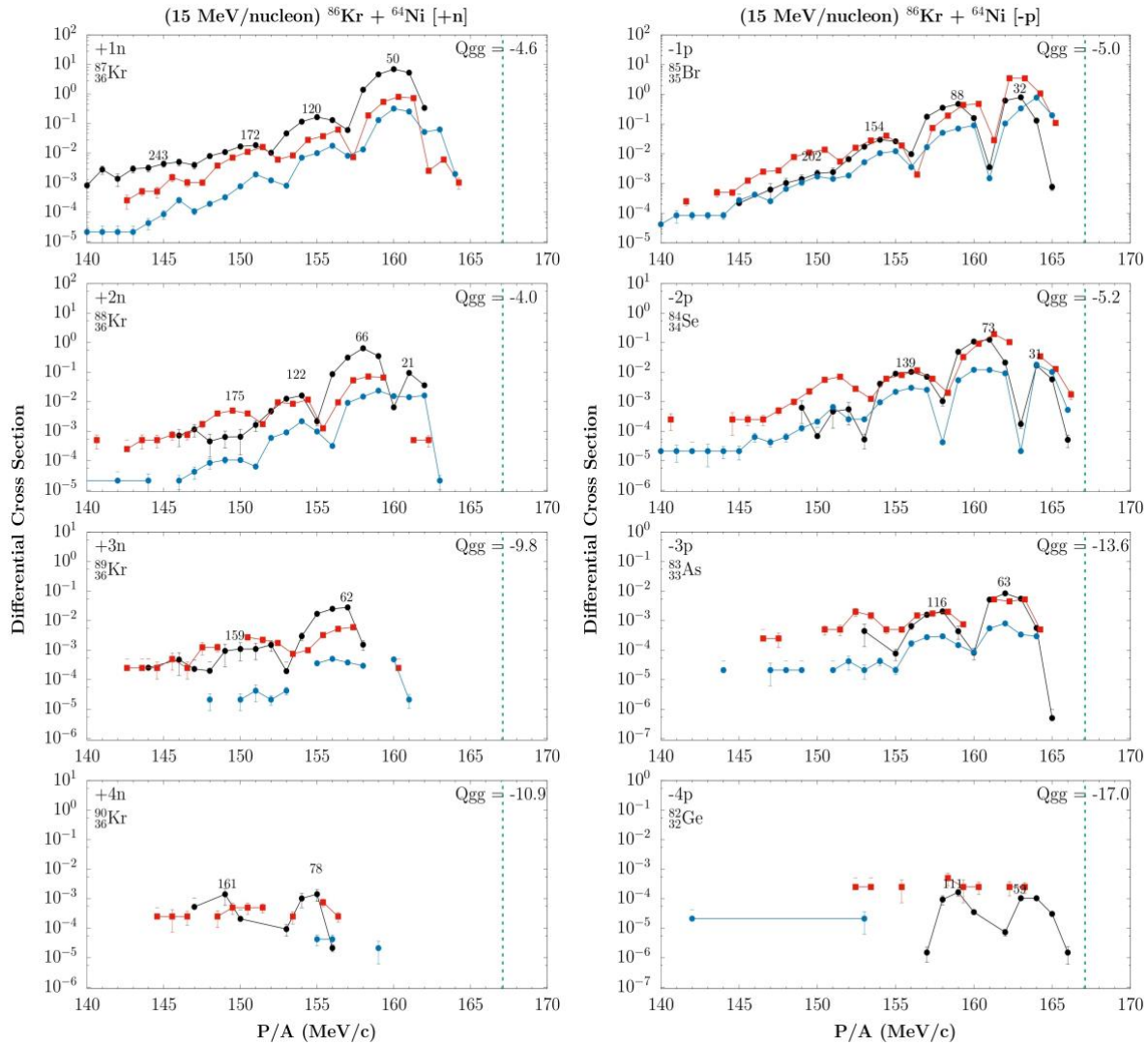


Figure 2. Momentum per nucleon distributions of ejectiles from neutron pickup (left) and proton removal channels (right) from $^{86}\text{Kr} + ^{64}\text{Ni}$ (15 MeV/nucleon). y-axis units: $(d^2\sigma/d(p/A)d\Omega - [\text{mb}/(\text{MeV}/\text{c})\text{msr}])$. Both panels: Experimental data: closed (black) circles. Numbers on top of peaks: Total excitation energy of dinuclear (quasitarget-quasiprojectile) system. DIT calculations closed (blue) circles. CoMD calculations closed (red) squares. The vertical dashed (green) line is the p/A of the projectile.

Multiple Charge Exchange Channels

Finally, as for the multiple exchange channels (-1n+1n), (-2p+2n) in Fig. 4 we once more observe that the DIT calculation does not describe the data adequately. The CoMD calculation again appears to

describe the broader peaks in a more sufficient way, even though it is lower than the data in the quasielastic region.

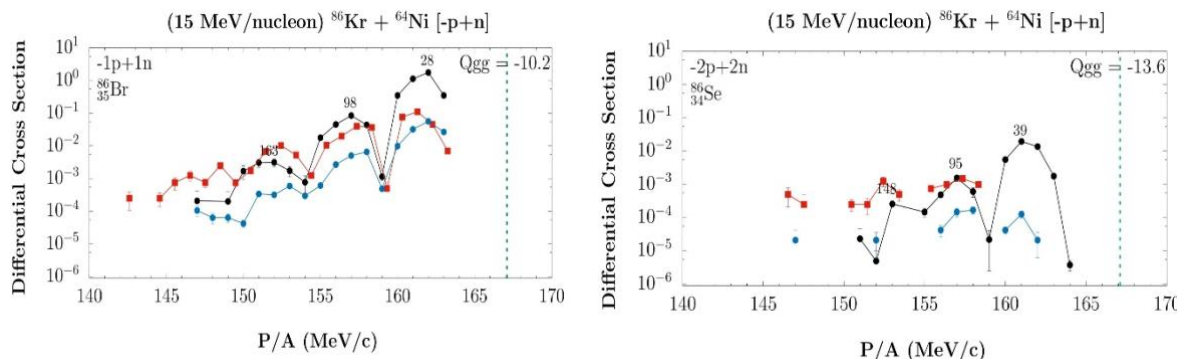


Figure 3. Momentum per nucleon distributions of ejectiles from multiple charge exchange channels from $^{86}\text{Kr} + ^{64}\text{Ni}$ (15 MeV/nucleon). y-axis units: $(d^2\sigma/d(p/A)d\Omega) - [\text{mb}/(\text{MeV}/\text{c})\text{msr}]$. Both panels: Experimental data: closed (black) circles. Numbers on top of peaks: Total excitation energy of dinuclear (quasitarget - quasiprojectile) system. DIT calculations closed (blue) circles. CoMD calculations closed (red) squares. The vertical dashed (green) line is the p/A of the projectile.

CONCLUSION- DISCUSSION

In this contribution, we presented part of our systematic research on peripheral reactions in the Fermi energy region. Experimental momentum per nucleon distributions on various channels from the reaction $^{86}\text{Kr} + ^{64}\text{Ni}$ at 15 MeV/nucleon were compared with DIT and CoMD calculations. Overall, the CoMD model appears to provide rather satisfactory results compared to the DIT model. Since CoMD is a microscopic model, it may allow improvements through proper optimization of appropriate parameters that describe the effective nucleon-nucleon interaction.

Regarding our future steps, we plan to investigate various reaction channels that may lead to the production of rare neutron rich nuclei. Furthermore, we intend to further adjust the different parameters of the CoMD model in order to describe the experimental data more adequately. Through our continued efforts [2,13-15] in studying multinucleon transfer reactions near the Fermi Energy, we expect to obtain valuable information on the reaction mechanisms in this energy region and apply this knowledge toward the production of neutron-rich nuclides.

References

- [1] G.G. Adamian et al., Eur. Phys. J. A 56, 47 (2020); doi: 10.1140/epja/s10050-020-00046-7
- [2] J. Diklić et al., Phys. Rev. C 107, 014619 (2023); doi: 10.1103/PhysRevC.107.014619
- [3] T. Mijatovic, Front. Phys. 10, 965198 (2022); doi: 10.3389/fphy.2022.965198
- [4] S. Heinz, H.M. Devaraja, Eur. Phys. J. A 58, 114 (2022); doi: 10.1140/epja/s10050-022-00771-1
- [5] V.V. Desai et al., Eur. Phys. J. A 56, 150 (2020); doi: 10.1140/epja/s10050-020-00154-4
- [6] O. Fasoula et al., HNPS Adv. Nucl. Phys. 29, 38 (2023); doi: 10.12681/hnpsanp.5089
- [7] G.A. Soulis et al., Phys. Rev. C 84, 064607 (2011); doi: 10.1103/PhysRevC.84.064607
- [8] L. Tassan-Got, C. Stephan, Nucl. Phys. A 524, 121 (1991); doi: 10.1016/0375-9474(91)90019-3
- [9] M. Papa, T. Maruyama, A. Bonasera, Phys. Rev. C 64, 024612 (2001); doi: 10.1103/PhysRevC.64.024612
- [10] M. Papa, G. Giuliani, A. Bonasera, J. Comput. Phys. 208, 403 (2005); doi: 10.1016/j.jcp.2005.02.032
- [11] R.J. Charity et al., Nucl. Phys. A 483, 371 (1988); doi: 10.1016/0375-9474(88)90542-8
- [12] R.J. Charity, Phys. Rev. C 58, 1073 (1998); doi: 10.1103/PhysRevC.58.1073
- [13] P.N. Fountas et al., Phys. Rev. C 90, 064613 (2014); doi: 10.1103/PhysRevC.90.064613
- [14] K. Palli et al., EPJ Web of Conf. 252, 07002 (2021); doi: 10.1051/epjconf/202125207002
- [15] S. Koulouris et al., Phys. Rev. C 108, 044612 (2023); doi: 10.1103/PhysRevC.108.044612